2014 International Conference on Unmanned Aircraft Systems (ICUAS)
May 27-30, 2014. Orlando, FL, USA

A Flight Control System Design for Highly Unstable Unmanned Combat Aerial Vehicles

Jiwon Jung, Yeunduk Jung, Dongil You, and David Hyunchul Shim

Abstract— This study proposes a flight control system for tailless unmanned combat aerial vehicles (UCAVs) and applies it to a representative example: the UCAV1303, an unstable blended wing body (BWB) aircraft. The UCAV1303 has no tail wing and a large sweepback angle, as a result of which it shows highly nonlinear aerodynamic characteristics such as wing rock and the pitch break phenomenon. In particular, in the latter, the pitching moment of an aircraft increases with the angle of attack, causing it to pitch up rapidly and then stall. In this study, an L_1 adaptive controller is designed for the UCAV1303 to accommodate and be robust to the pitch break phenomenon, which is used to model uncertain aerodynamics.

Furthermore, a moving wing fence is proposed for realizing good stability and performance at a high angle of attack. It delays flow separation and aerodynamic stalling, thereby improving the effectiveness of the wing and other control surfaces at a high angle of attack. Under normal or level flight conditions, during which the angle of attack is low, it may negatively affect the aircraft performance because it increases the radar cross section and parasitic drag. A series of flight tests were performed to validate the proposed controller and moving wing fence. The former is robust to model uncertain aerodynamics, and the latter prevented the pitch break phenomenon at a high angle of attack and afforded an adequate margin between the initial and the pitch break regions.

I. INTRODUCTION

Unmanned combat aerial vehicles (UCAVs) are finding increasing use in the military. For a UCAV to be effective, it must have long endurance and low observability. However, a UCAV with a stealthy design, like many other modern aircraft, is likely to be aerodynamically unstable.

As a representative example of a UCAV, we investigate the UCAV1303, a tailless, unstable blended wing body (BWB) aircraft. The UCAV 1303 has no tail wing and a large sweepback angle, as a result of which it shows highly nonlinear aerodynamic characteristics such as the pitch break phenomenon. In particular, the latter causes the pitching moment of an aircraft increase with the angle of attack, causing it to pitch up rapidly and then stall.

Atkinson *et al.* [1], Brett *et al.* [2], Petterson [3], and Khalid *et al.* [4] have conducted computational fluid dynamics analyses of the UCAV1303 and its vortex lift and pitch break phenomenon. McLain [5] conducted a water tunnel test to measure the aerodynamic coefficients and conducted flow visualization. Furthermore, Patel *et al.* [6] designed an L_1 adaptive controller for a Multi Input Multi Output(MIMO) open loop unstable unmanned military aircraft to accommodate and be robust to actuator failures as well as to the pitch break uncertainty that is used to model uncertainties. Tyler Leman *et al.* [7] designed an L_1 adaptive controller to model the X-48B BWB aircraft. Lavretsky and Wise [8] applied model reference adaptive control (MRAC) to model the X-45A, an aerodynamically unstable UCAV.

In this study, we design a flight control system for the UCAV1303. A wind tunnel test was conducted to investigate its aerodynamic characteristics with active flow control using a micro vortex generator (MVG). In the wind tunnel test, the MVG delayed flow separation, thus delaying the pitch break phenomenon, and in the flight test, it improved performance and stability.

Figure 1. UCAV 1303 test flight.

*Resrach supported by ABC Foundation.

J. Jung is with the Department of Aerospace Engineering, KAIST, Daejeon, South Korea (phone: +82-42-350-3764; fax: +82-42-350-3710; e-mail: jeongjiwon@kaist.ac.kr).

Y. Jung, D. You and D. H. Shim are with the Department of Aerospace Engineering, KAIST, Daejeon, South Korea (e-mail: jyd28@kaist.ac.kr, diyou@fdcl.kaist.ac.kr, hcshim@kaist.ac.kr)

In order to control pitch break at a high angle of attack, L_1 adaptive control was implemented using baseline proportional-derivative (PD) control. An L_1 adaptive controller was applied to nonlinear simulation, and the results show that the system is BIBO stable and non-minimum phase, indicating that it can be used to solve the high angle of attack problem. The controller can track a desired attitude despite uncertainties and unexpected pitch motions. Its performance was validated through numerical simulations and a flight test.

II. UCAV1303

A. *Aerodynamic Characteristics of UCAV1303*

The UCAV1303 is a representative model of a UCAV platform. It is a tailless, unstable BWB aircraft with a leading edge sweep angle of 47°. It shows highly nonlinear aerodynamic characteristics such as wing rock and the pitch break phenomenon. In particular, in the latter, the pitching moment of an aircraft increases, causing it to pitch up rapidly and then stall. The vortical flow over highly swept-back or delta wings at a high angle of attack is highly nonlinear owing to vortex asymmetry, stream-wise and cross-flow separation, and/or vortex breakdown. A wind tunnel test was conducted to investigate its aerodynamic characteristics with active flow control using a MVG. Fig. 3 showed that pitch break occurs at an angle of attack of ~10° and the MVG delayed flow separation, thus delaying the pitch break by ~5°.

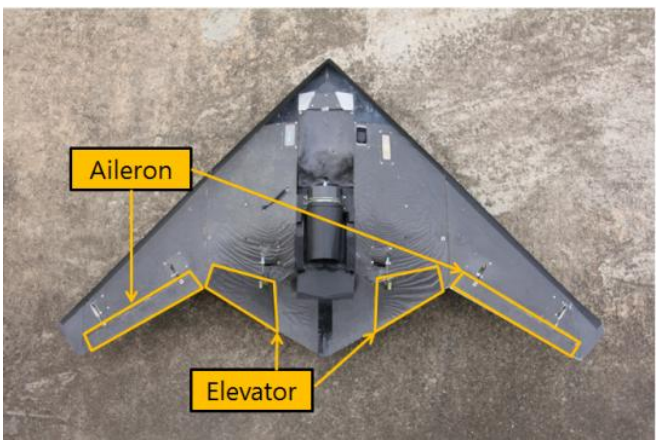

Figure 2. Flight test platform UCAV1303.

B. *Airframe and Control Surfaces*

Fig. 2 shows the custom-designed UCAV1303 flight test platform. It has a nominal gross weight of 8 kg and wing span of 2 m. As control surfaces, it has two inboard and outboard elevons and a moving fence. It is powered by an electronic ducted fan unit.

A wing fence is a flat plate that is attached perpendicular to the wing in line with the free stream air flow. The vortex breakdown at the wing root and the spanwise flow near the leading edge go to the wing tip, causing the outboard wing to stall and the outboard control surface to lose control. A wing fence attached in the path of the spanwise flow obstructs it and thus prevents wing stall. A wing fence effectively maintains control effectiveness at a high angle of attack. A wing fence is used for improving stability and performance, particularly at high angles of attack, such as those during take-off, landing, and initial climbing. Under normal or level flight conditions, during which the angle of attack is low, a wing fence may negatively affect the aircraft performance because it increases the radar cross section and parasitic drag. The former is particularly undesirable for the UCAV1303, which, like many other modern aircraft, is intended to be stealthy.

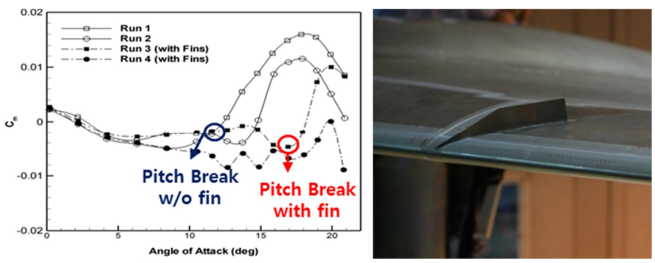

Figure 3 Pitching moment with/without MVG


Figure 4. UCAV1303 fitted with a MVG.


Figure 5. UCAV1303 fitted with a moving wing fence.

To overcome these problems, we developed a moving wing fence as Fig. 5 and attached it to the mid-span. Two servo motors rotate about an axis parallel to the wing span to move the wing fence up and down. At a high angle of attack, it moves up to prevent wing stall and maintain control surface effectiveness; under normal flight or level flight conditions, it moves down to reduce the radar cross section.

We conducted flight tests of the UCAV1303 without and with the moving fence. In the former case, pitch break occurred during take-off and initial climbing; this reduced the outboard control surface effectiveness, making the aircraft difficult to control and causing it to spin and crash. In the latter case, pitch break was prevented at a high angle of attack, and an adequate margin was afforded between the initial and the pitch break regions.

B. *Avionics*

Fig. 6 shows the hardware setup of the UCAV1303 for the flight test. Its avionics consists of a flight control computer (FCC), an inertial measurement unit (IMU), a GPS sensor, and a PWM generation board. The FCC is constructed using Gumstix Verdex pro XL6P; it is lightweight (8 g) and compact (80 mm × 20 mm), and it features low energy consumption and high processing speed. It is suitable for application to the experimental flight control algorithm for our aircraft.

A GPS-aided inertial navigation system (INS) based on an extended Kalman filter (EKF) is used. The GPS is a single U-Blox EVK-5H that nonetheless offers excellent signal tracking performance and high reliability.

The vehicle acceleration and angular rate measured using the AHRS are read by an in-flight computer via RS232 serial ports and processed by a

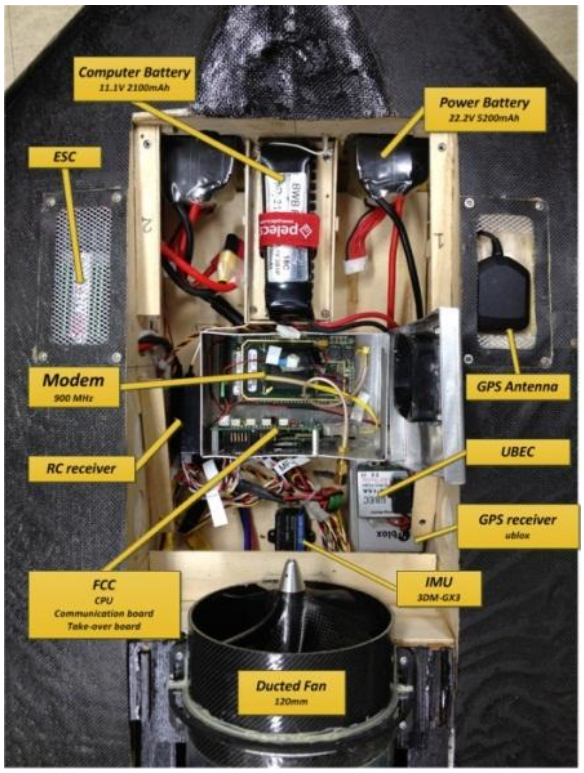

Figure 6. Hardware setup for UCAV1303.

navigational routine at 100 Hz to calculate the aircraft's attitude, velocity, position, and heading. The error of the inertial measurement sensor is estimated and compensated using EKF processing at 5 Hz when the GPS calculates the aircraft position.

III. Flight Control System

In this section, the L_1 adaptive control design for tracking of reference command is presented. The L_1 adaptive control law is similar to the model reference adaptive control (MRAC) which includes the output predictor, parameter estimator, and low-pass filter as shown in Figure 6. The L_1 adaptive controller uses a large adaptive control gain for fast adaptation and a low-pass filter is used to prevent performance degradation in the transient

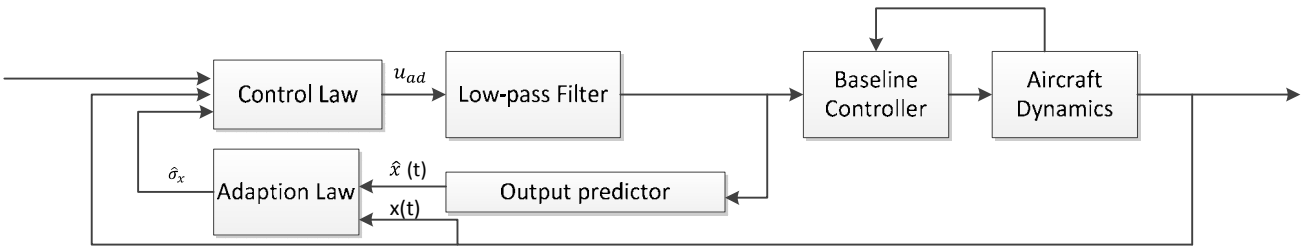

Figure 7. Output feedback based L_1 adpative control loop.

response. The pitch adaptation gain was designed relatively larger to cope with the model uncertainties due to the pitch break phenomenon at a high angle of attack. L_1 adaptive controller also eliminates the need for additional gain scheduling as it can adeptly cope with the perturbed dynamics during the flight [9-10].

A. L_1 Adaptive Control

The L_1 adaptive control is developed for a single input single output system. The dynamics of the error can be described as follows:

$$y(s) = A(s)(u(s) + d(s)) \tag{1}$$

where $u(s)$ and $y(s)$ are the input and the output transfer function of the system, respectively. $A(s)$ and $d(s)$ are a transfer function that is strictly not properly known and a Laplace transform of the system uncertainties, respectively. The adaptive controller can compensate for uncertainties, and it makes the system track the desired command by following the reference model. Here, the reference model and the dynamics of the error are described as

$$y(s) = M(s)(u(s) + \sigma(s)) \tag{2}$$

Here, $\sigma(s)$ is an unknown signal, and it is derived as

$$\sigma(s) = \frac{\big(A(s) - M(s)\big)u(s) + A(s)d(s)}{M(s)}. \tag{3}$$

In order to track the desired reference value where the output $\hat{y}(t)$ is bounded using the L_1 adaptive controller an output predictor, an adaptation law, and a control law are required. The output predictor can be expressed as

$$\begin{aligned} \dot{\hat{\mathbf{x}}}(t) &= -\mathbf{A}_\mathbf{m}\hat{\mathbf{x}}(t) + \mathbf{B}_\mathbf{m}(u_{ad}(t) + \hat{\boldsymbol{\sigma}}(t)), \quad \hat{\mathbf{x}}(0) = \mathbf{0}, \\ \hat{y}(t) &= \mathbf{C}_\mathbf{m}\hat{\mathbf{x}}(t) \end{aligned} \tag{4}$$

where $\mathbf{A}_\mathbf{m}$, $\mathbf{B}_\mathbf{m}$, and $\mathbf{C}_\mathbf{m}$ are the minimal realizations of the desired model $M(s)$, and $\hat{\boldsymbol{\sigma}}(s)$ is the adaptive parameter.

The adaptive parameter is calculated using the following adaptive law.

$$\begin{aligned} &\hat{\boldsymbol{\sigma}}(t) = \hat{\boldsymbol{\sigma}}(iT_s), \qquad t \in \big[iT_s, (i+1)T_s\big), \\ &\hat{\boldsymbol{\sigma}}(iT_s) = -\boldsymbol{\Phi}^{-1}(T_s)\boldsymbol{\mu}(iT_s),\ i = 0,1,2,\cdots, \end{aligned} \tag{5}$$

$\boldsymbol{\Phi}(T_s)$ is defined as

$$\boldsymbol{\Phi}(T_s) = \int_0^{T_s} e^{\boldsymbol{\Lambda}\mathbf{A}_\mathbf{m}\boldsymbol{\Lambda}^{-1}(T_s-\tau)}\boldsymbol{\Lambda}\, d\tau \tag{6}$$

Here, $\boldsymbol{\mu}(iT_s)$ can be expressed as

$$\boldsymbol{\mu}(iT_s) = e^{\boldsymbol{\Lambda}\mathbf{A}_\mathbf{m}\boldsymbol{\Lambda}^{-1}T_s}\mathbf{1}_\mathbf{1}\tilde{y}(iT_s), \quad i = 0,1,2,..., \tag{7}$$

Here, $\mathbf{1}_\mathbf{1}$ may represent $\mathbf{1}_\mathbf{1} = [1,0,\cdots,0]^T$. Let $\tilde{y}(t) = \hat{y}(t) - y(t)$ as derived from the Lyapunov equation. $\mathbf{A}_\mathbf{m}$ is the reference model of the adaptive controller, and it can be defined by the Hurwitz matrix. Hence, the Lyapunov equation can be expressed as

$$\mathbf{A}_\mathbf{m}^\mathbf{T}\mathbf{P} + \mathbf{P}\mathbf{A}_\mathbf{m} = -\mathbf{Q}, \qquad \text{where} \qquad \mathbf{Q} = \mathbf{Q}^\mathbf{T} > 0 \tag{8}$$

If $\sqrt{\mathbf{P}}$ exists, then the null space $\mathbf{D}$ can be defined as follows:

$$\mathbf{D}\left(\mathbf{C}_\mathbf{m}\left(\sqrt{\mathbf{P}}\right)^{-1}\right)^T = \mathbf{0} \tag{9}$$

Here, $\boldsymbol{\Lambda}$ is defined as

$$\boldsymbol{\Lambda} = \begin{bmatrix} \mathbf{C}_\mathbf{m} \\ \mathbf{D}\sqrt{\mathbf{P}} \end{bmatrix} \tag{10}$$

The control law $u_{ad}(s)$ is designed as follows:

$$u_{ad}(s) = C(s)r(s) - \frac{C(s)}{\mathbf{C}_\mathbf{m}^\mathbf{T}(\mathbf{sI} - \mathbf{A}_\mathbf{m})^{-1}\mathbf{B}_\mathbf{m}}\mathbf{C}_\mathbf{m}^\mathbf{T}(\mathbf{sI} - \mathbf{A}_\mathbf{m})^{-1}\hat{\boldsymbol{\sigma}}(s) \tag{11}$$

Here, $C(s)$ is the strictly proper low-pass filter and $r(s)$, the bounded reference input. The cutoff frequency of the low-pass filter is chosen based on the trade-off between the performance and the robustness of the L_1 adaptive controller.

In this study, the output feedback based L_1 adaptive controller is designed for the roll and pitch axes. The control objective is to reduce the attitude error to zero. Here, the reference model $M(s)$ is assumed to be a second-order system as follows:

$$M(s) = \frac{\omega_n^2}{s^2 + 2\omega_n\xi s + \omega_n^2} \tag{12}$$

where ω_n is the natural frequency and ξ, the damping ratio. The validity of the stability and guaranteed performance boundary values of the closed-loop reference system are given in [9]. This L_1 adaptive control law is integrated with the conventional PD controller as shown in Fig. 7.

IV. Simulation Result

The tracking performance of the baseline PD controller and L_1 adaptive controller in the presence of pitch break is compared. The latter was implemented to augment the UCAV1303 dynamic model.

To obtain the dynamic model for the UCAV1303, its aerodynamic characteristics should be known. The aerodynamic coefficients are modeled by AVL. The lifting surface model for the UCAV1303 as generated by AVL is shown in Fig. 8. The chord line indicates the reflex airfoil in the inboard body section and the linearly distributed twist angle in the outboard wing section, which is designed to guarantee static stability for a BWB aircraft without any control surface bias.

Furthermore, the data for the nonlinear longitudinal characteristics generated by the wind tunnel test in Fig. 8 were also obtained[2].

The L_1 adaptive controller augments the roll and pitch angle commands generated by the baseline PD controller to track the reference model dynamics. These reference models are of second order for the pitch and roll response. Fig. 9 shows the time history of the response to a pitch step command. Relative to the baseline PD controller, the L_1 adaptive controller largely reduces the overshoot in the pitch step command and tracks the reference model with rapid adaptation.

Figs. 10–11 show the benefits of the L_1 adaptive controller in the presence of pitch break. An unknown pitching moment is added to simulate pitch break uncertainty. Pitch break occurs at 7 s, as shown in Fig. 10. During pitch break, the PD controller shows poor performance; it cannot track the desired command well and shows a steady-state error. In comparison, the L_1 controller well adapts and tracks the desired command. Figs. 11 shows the time history of the response to a sinusoidal pitch input. Until 15 s, both controllers track the pitch angle command well. However, when pitch break occurs at 15 s, the PD controller has an offset to the pitch angle command whereas the L_1 adaptive controller quickly adapts and tracks the pitch angle command. Figs. 12–14 show the adaptation parameters. The L_1 adaptive parameters change and compensate for unstable pitching motions such as the pitch break phenomenon.

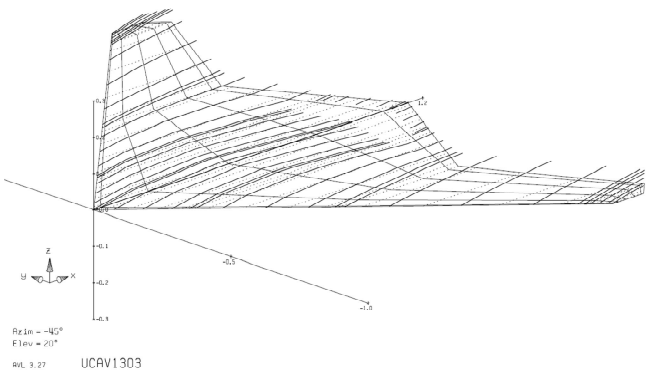

Figure 9. Vortex Lattice Model for UCAV1303 Platform

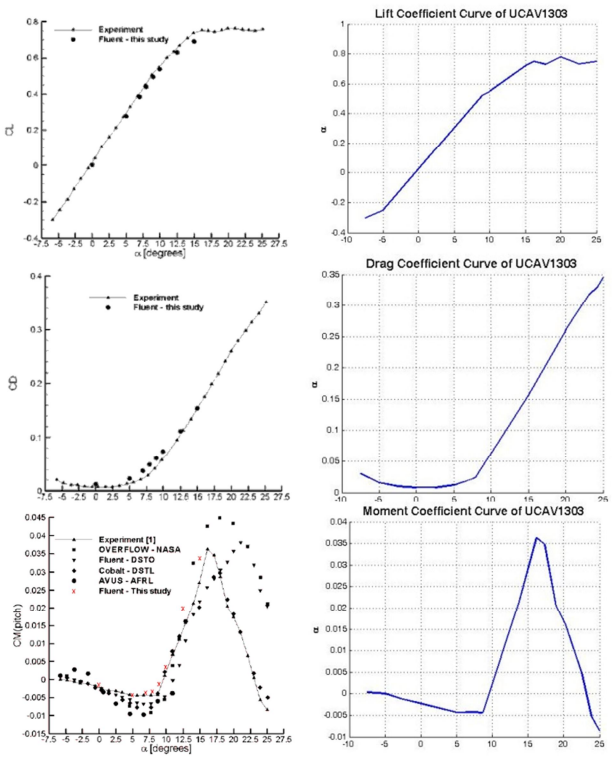

Figure 8. Coefficient of lift, drag and pitch of UCAV1303 Platform

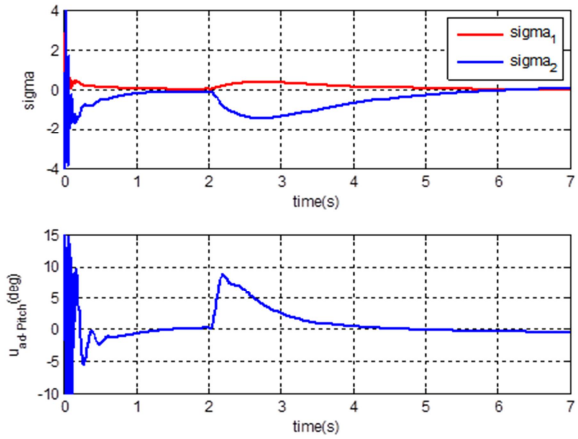

Figure 10. Adaptive parameters.

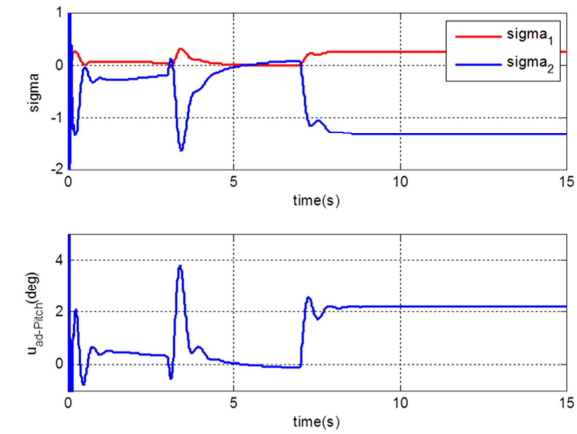

Figure 11. Adaptive parameters.

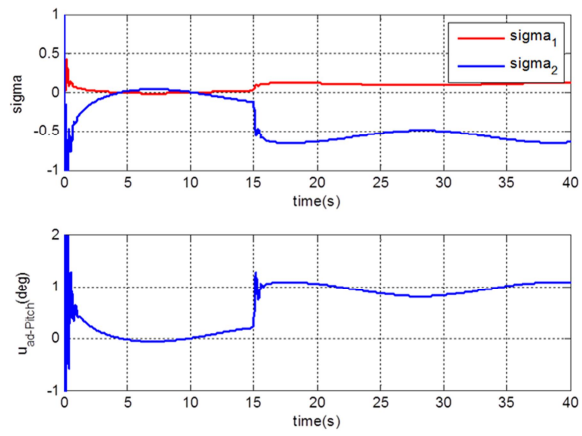

Figure 12. Adaptive parameters.

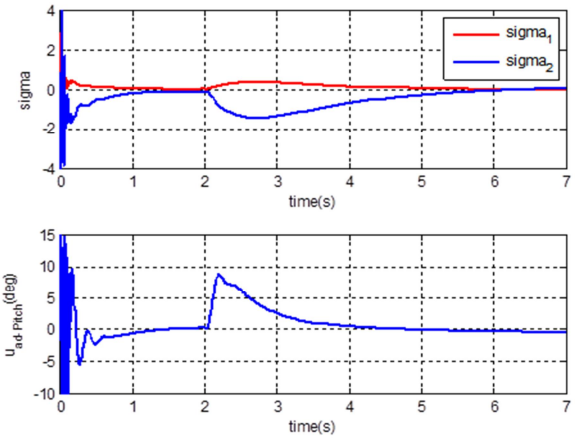

Figure 13. Adaptive parameters.

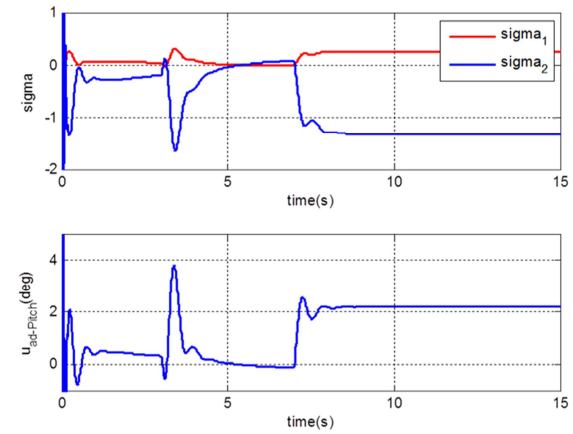

Figure 14. Adaptive parameters.

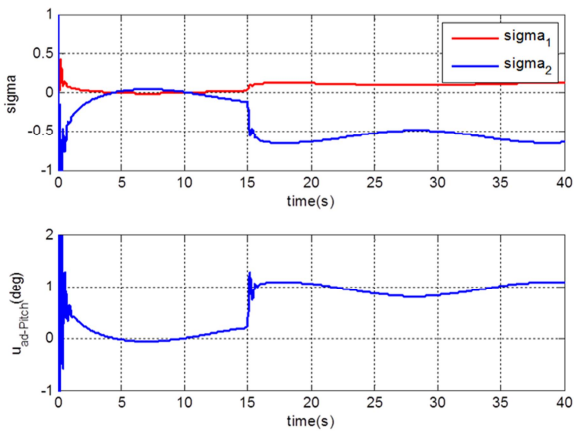

Figure 15. Adaptive parameters.

V. Experimental Result

The flight control system of the UCAV1303 platform with a moving wing fence was implemented and validated through flight tests.

During take-off and initial climbing, pitch break occurs. Because of the spanwise flow, the outboard control surface effectiveness is reduced, making the aircraft difficult to control. The use of a wing fence enabled the aircraft to take-off and land safely; during normal flight, the wing fence is moved down.

To control the pitch break at a high angle of attack, L_1 adaptive control was implemented with baseline PD control. The proposed controller can be used to solve the high angle of attack problem. It can track a desired attitude despite uncertainties and unexpected variations. Its performance has been validated through flight tests.

Fig. 16 shows the flight test result of the pitch angle, pitch rate, and elevator input; the L_1 adaptive controller tracks the desired command angle well. Fig. 18 shows the controller's adaptive parameters. They change and compensate for modeling errors and disturbances. The L_1 controller generates L1 commands that are provided as control inputs to the PD controller so that the aircraft can track the reference well.

Fig. 19 shows the flight test result of a sinusoidal pitch input. The L_1 controller tracks the desired command well. Fig. 21 shows that its adaptive parameters change rapidly. The L_1 controller generates L_1 commands that are provided as control inputs to the baseline PD controller to track the desired command so that the aircraft can track the sinusoidal input.

In a flight test, uncertainties such as pitch break and other disturbances may occur. Fig. 15 shows a comparison of the results of the PD controller and the L_1 controller. The PD controller shows poor performance for a sinusoidal input, as in the simulation result. In comparison, the L_1 controller tracks the desired command well. The pitch angle error of the PD controller is ~10°, whereas that of the L_1 controller is very small. Overall, the adaptive controller shows better performance in the flight test.

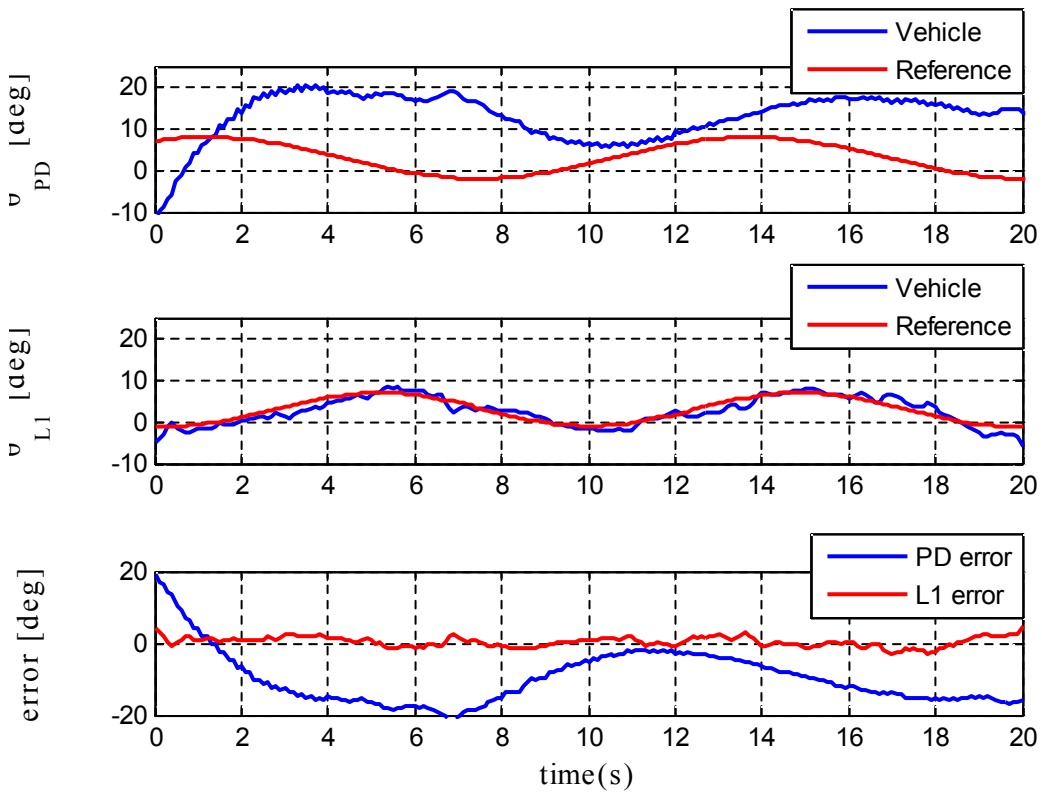

Figure 16. Pitch response to sinusoidal input (PD controller and L_1 controller).

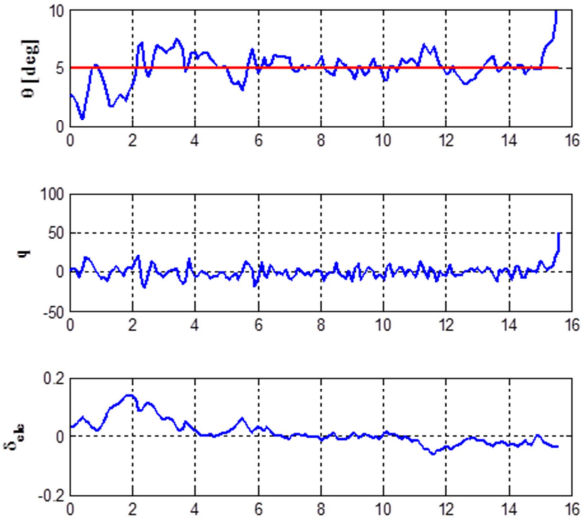

Figure 17. Pitch response of L_1 adaptive controller.

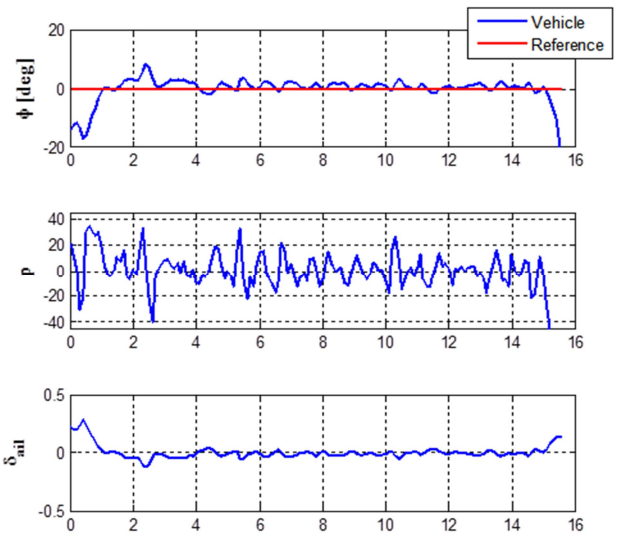

Figure 18. Roll response of L_1 adaptive controller.

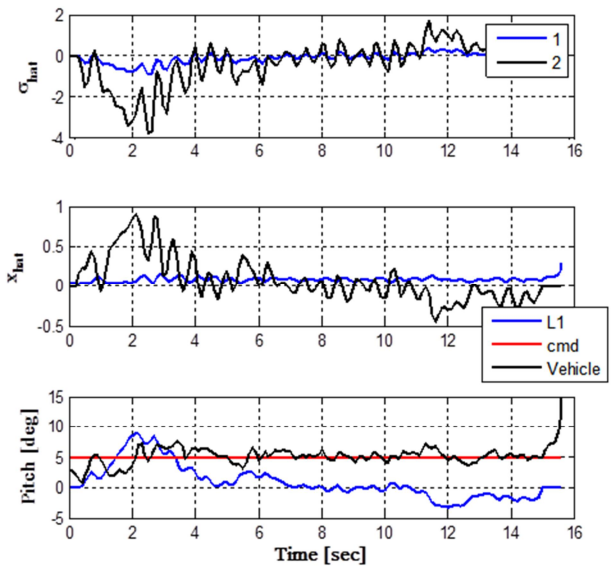

Figure 19. Adaptation parameters.

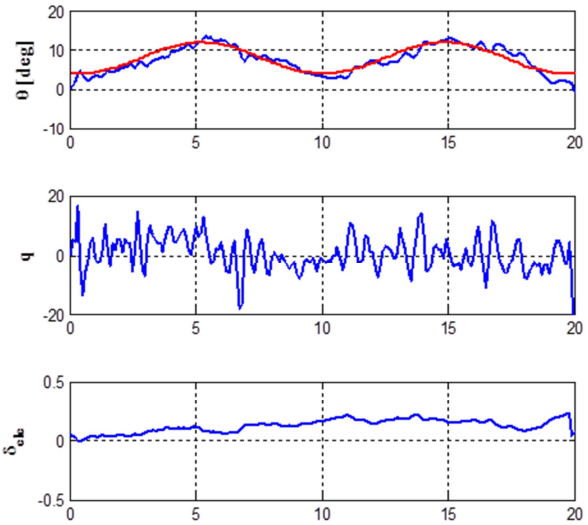

Figure 20. Pitch response of L_1 adaptive controller.

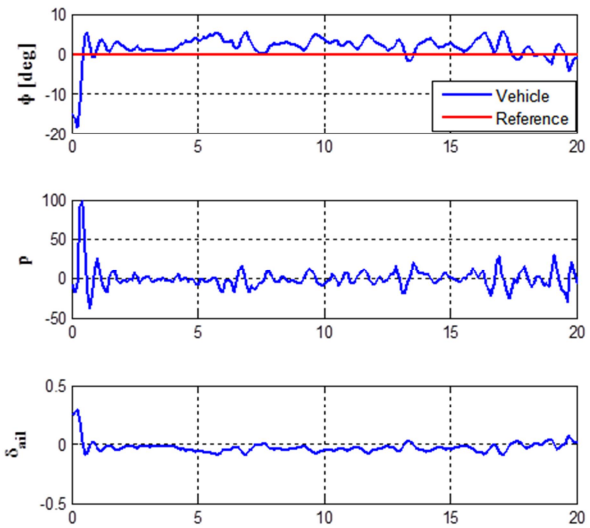

Figure 21. Roll response of L_1 adaptive controller.

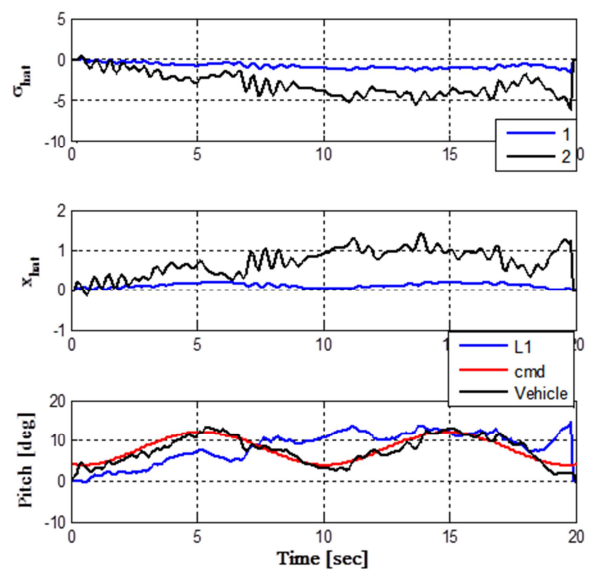

Figure 22. Adaptation parameters.

VI. Conclusion

This study presents a control system design for tailless UCAVs and verifies the same through experiments conducted using the UCAV1303, a tailless, unstable BWB aircraft. A moving wing fence is applied to the UCAV1303 at the mid-span to prevent the pitch break phenomenon at a high angle of attack and to afford an adequate margin between the initial and the pitch break regions.

In the proposed flight controller, a conventional PD controller is augmented with an L_1 adaptive controller to handle uncertainties such as the pitch break phenomenon. The proposed controller was implemented using an in-house flight controller built on a small embedded computer with a lightweight INS and GPS. Its performance has been validated through numerical simulations and flight tests. As a result, the proposed controller can be used to solve the high angle of attack problem. It can track a desired attitude despite uncertainties and unexpected variations.

Acknowledgment

This work was supported by Agency for Defense Development(ADD) under the contract UD130041 JD and UE124026JD

References

[1] M. Atkinson and F. Ferguson. (2006). "A Computational Fluid Dynamics Investigation of the 1303 UCAV Configuration with Deployable Rao Vortex Flaps", 44th AIAA Aerospace Sciences Meeting, 2006, Nevada, USA

[2] J. Brett, L. Tang, N. Hutchins, A. Valiyff and A. Ooi. (2010). "Computational Fluid Dynamics Analysis of the 1303 Unmanned Combat Air Vehicle", 17th Australasian Fluid Mechanics Conference, Austrailia, 2010 pp. 341–344.

[3] K. Petterson. (2006). "CFD Analysis of the Low-Speed Aerodynamic Characteristics of a UCAV", 44th AIAA Aerospace Sciences Meethign, 2006, Nevada, USA.

[4] M. Khalid, W. Yuan and F. Zhang. (2008). "A CFD Study of UCAV 1303 Baseline Model at Cruise Mach Numbers", Proc. 26th Congress of Int. Council of the Aeronautical Sciences, Alaska, pp. 2.5.1-1–2.5.1-10.

[5] B. K. McLain. (2009). "Steady and Unsteady Aerodynamic Flow Studies over a 1303 UCAV Configuration", Master Thesis, Dept. Mechanical and Astronautical Eng., Naval Postgraduate School, California, 59 pages.

[6] Vijay V. Patel, Chengyu Cao, Naira Hovakimyan, Kevin A. Wise and Eugene Lavretsky (2007) L_1 adaptive controller for Tailless Unstable Aircraft", American Control Conference, New York, USA, 2007

[7] T. J. Leman. (2011). "L_1 Adaptive Control Augmentation System for the X-48B Aircraft", M.S. Thesis, University of Illinois at Urbana-Champaign, Urbana, Illinois, 42 pages.

[8] Lavretsky, E. Wise, K., Adaptive Flight Control for Manned/Unmanned Military Aircraft, Amer. Contr. Conf., 2005.

[9] Xargay, E., Hovakimyan, N. and Cao, C., "Benchmark Problems of Adaptive Control Revisited by L_1 Adaptive Control," 17th Mediterranean Conference on Control & Automation, Thessaloniki, Greece, pp.31~36. 2009.

[10]Hovakimyan, N. and Cao, C., L1 Adaptive Controller Theory Guaranteed Robustness with Fast Adaptation, Advances in Design and Control, 2010.